The Radical Anion of Tetraphenylene Revisited

Markus Scholz and Georg Gescheidt *
Institut für Physikalische Chemie, Universität Basel, Klingelbergstrasse 80, CH-4056 Basel, Switzerland

The tetraphenylene radical anion ($2^{\bullet -}$) generated by Na, K and Cs reduction in tetrahydrofuran and 2-methyltetrahydrofuran has been investigated by EPR/ENDOR spectroscopy. The results clearly establish that the decrease of the molecular symmetry of $2^{\bullet -}$ from D_{2d} to C_{2v} detected upon exhaustive reduction arises from ion-pair formation. This finding unequivocally rules out the assumption stated in previous papers that the EPR spectra mirroring the lower symmetry originate in a bis(biphenylene)-like geometry of $2^{\bullet -}$

When electrons are transferred to a neutral molecule, the change of the electronic structure may significantly alter the shape of the reduced species.[1] One of the early examples in this respect was cyclooctatetraene (**1**).[2] The neutral **1**, an 8 π electron system, possesses a 'buckled' geometry of D_{2d} symmetry.[3] For the dianion, 1^{2-}, a 10 π electron system obeying the Hückel rule, a planar geometry has been established by X-ray crystallography.[4] Analogous behaviour has also been reported for mono- or di-[*a*,*e*]benzannellated cyclooctatetraenes based on electrochemical measurements and NMR spectroscopy.[5] EPR studies corroborate that the one-electron reduced species, the radical anions, have geometries[6] almost identical with the dianions.

The tetrabenzo derivative of **1**, tetraphenylene (**2**), exhibits a tub-shaped geometry;[7] however, the steric congestion by the *ortho* H-atoms and angle strain impedes the molecule from adopting a planar conformation after electron transfer. A few years ago, 2^{2-} was investigated by NMR spectroscopy.[8] It was found that the molecular symmetry had decreased from D_{2d} to C_2 and thus 2^{2-} was described as two coupled biphenyl subunits 'with the localisation of the excess charge in one entity' (Fig. 1).

The radical anion $2^{\bullet -}$ was generated *via* two procedures:[9,10] the first was one-electron reduction with K-metal of neutral **2**, and the second technique involved formation of the dianion 2^{2-} followed by photo-oxidation (Scheme 1). Remarkably, the

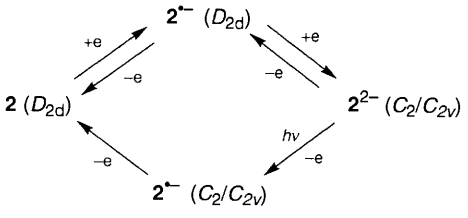

Scheme 1

EPR spectra obtained in ref. 9 were specific to the method employed. Whereas one-electron reduction led to EPR spectra indicating D_{2d} symmetry of $2^{\bullet -}$, the species generated *via* photo-oxidation gave rise to EPR spectra mirroring a symmetry reduction to C_2 (or C_{2v}).† Thus it was concluded that the radical anion of tetraphenylene **2** occurs in two forms depending on the procedure of generation: one structure having equivalent symmetry to the neutral molecule, the other, with lowered symmetry, resembling the dianion-type structure (Fig. 1).

† The multiplicities of the proton-coupling constants given by Huber[9] were claimed to represent C_2 symmetry; however, these multiplicities are in line with C_{2v} symmetry as well.

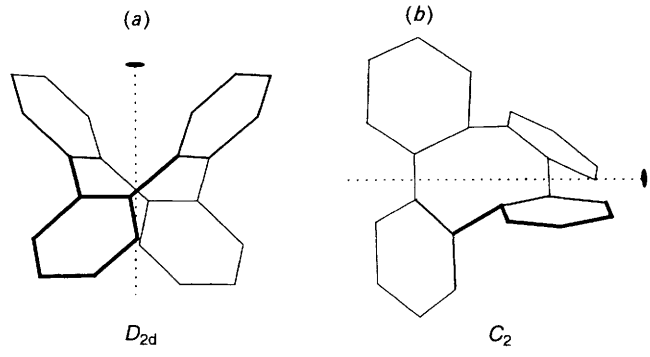

Fig. 1 Geometries of **2** ($2^{\bullet -}$, 2^{2-}): (*a*) D_{2d} symmetry of **2** and $2^{\bullet -}$; (*b*) C_2 of $2^{\bullet -}$ and 2^{2-} as deduced from EPR and NMR spectra in refs. 8, 9 and 10. The dashed lines indicate the C_2 axes. Hydrogens and double bonds are omitted for clarity.

More recently, it was pointed out that such a symmetry reduction may alternatively be connected with the formation of a contact ion pair in which the association with the counter cation leads to a decrease of the symmetry.[11] To determine whether such ion-pair and solvation effects play an important role for the detection of C_2 (or C_{2v}) symmetric $2^{\bullet -}$, we employed Cs metal in addition to K for the reduction reactions. The Cs^+ ion should form ion pairs very similar to those of K^+. The advantage of the Cs nucleus is the higher isotropic hyperfine coupling constant for unit spin density compared with K[12] [ratio: $a(^{39}K)/a(^{133}Cs)$ 1:11]. This leads to more easily detectable hyperfine interactions of the Cs^+ counterion under conditions where the K^+ ion is not discernible. As the solvents, dimethoxyethane (DME), tetrahydrofuran (THF) and 2-methyltetrahydrofuran (MTHF) were employed. The decreasing solvation power DME > THF > MTHF allows the study of different stages of ion-pair formation.[13]

Results and Discussion

Reduction Behaviour.—In DME as the solvent, reduction with K or Cs led to the well known EPR spectrum of $2^{\bullet -}$. Its pattern consists of a nonet of nonets with hydrogen hyperfine coupling constants, a_H, of *ca.* 0.130 mT [H–C(2,3,6,7,10,11,-14,15)] and 0.012 mT [H–C(1,4,5,8,9,12,13,16)][9–11] [identical with that shown in Fig. 2(*a*)].

With the use of THF, however, the shapes of the EPR spectra become dependent upon the period of reduction, *i.e.*, the period of time in which the solution of **2** is in contact with the metal mirror. After *ca.* 5–10 s of reduction with K or Cs at 193 K, the typical nonet of nonets EPR signal (see above) is observed (Fig. 2). Upon longer contact with the K mirror, the relative

Table 1 Proton- and metal-hyperfine coupling constants (mT)[a] of $2^{\bullet -}$

Solvent/counterion (T/K)	g Factor	Proton position 1,4,9,12	5,8,13,16	2,3,10,11	6,7,14,15	Metal	Symmetry[b]
DME/K^+ (203)	2.002 79	+0.012	+0.012	−0.130	−0.130		D_{2d} (100%)
DME/Cs^+ (203)	2.002 80	+0.012	+0.012	−0.131	−0.131		D_{2d} (100%)
THF/Cs^+ (178)	2.002 83	+0.017	+0.017	−0.131	−0.131		D_{2d} (75%)
	2.002 30	+0.013	c	−0.165	−0.097	0.120	C_{2v} (25%)
THF/Cs^+ (198)		+0.017	+0.017	−0.131	−0.131		D_{2d} (62%)
		+0.013	c	−0.165	−0.097	0.116	C_{2v} (38%)
THF/Cs^+ (208)		+0.017	+0.017	−0.130	−0.130		D_{2d} (50%)
		+0.013	c	−0.165	−0.097	0.115	C_{2v} (50%)
THF/Cs^+ (223)		+0.015	+0.015	−0.130	−0.130		D_{2d} (42%)
		+0.013	c	−0.165	−0.097	0.112	C_{2v} (58%)
MTHF/K^+ (198)	2.002 83	+0.018	+0.018	−0.132	−0.132		D_{2d} (100%)
MTHF/K^+ (203)[d]		+0.013	c	−0.165	−0.097	<0.01	C_{2v} (100%)
MTHF/Cs^+ (196)	2.002 28	+0.013	c	−0.167	−0.095	0.119	C_{2v} (100%)

[a] Experimental error, ±0.001 mT for the coupling constants and ±0.000 06 for the g factors; the signs of a_H were obtained from general-TRIPLE measurements under the assumption that the major a_H is negative; the sign of a_{Cs} can only be derived from its temperature behaviour: the decrease of a_{Cs} with increasing temperature was in line with a negative sign; for numbering, see Fig. 7. [b] The percentages of the spectral components are based on simulations. [c] Because of the broad lines in the EPR spectra, the multiplicities of the a_H of 0.013 mT cannot be determined (4 H, or 8 H). [d] Spectrum obtained after exhaustive reduction followed by photo-oxidation as described in ref. 9.

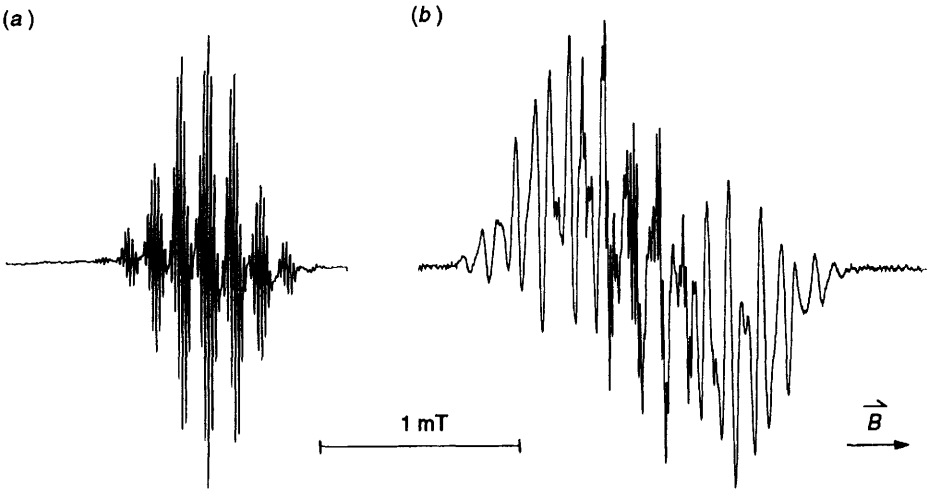

Fig. 2 EPR spectra of $2^{\bullet -}$ depending on the period of reduction (solvent, THF; counterion, Cs^+; T = 193 K): (*a*) after 5 s; (*b*) after 3 h

intensities of the central lines decrease whereas the high- and low-field wings of the spectra increase.

For Cs, not only the line pattern but also the widths of the EPR spectra change significantly. This is illustrated in Fig. 2 where the EPR spectra of $2^{\bullet -}$–Cs^+–THF after *ca.* 5 s and 3 h of contact with the Cs mirror at 193 K are shown. Upon increasing the reaction time the EPR signal becomes composed of two superimposed spectra, one being identical with the original spectrum of $2^{\bullet -}$, the second being broader by *ca.* 0.8 mT due to a hyperfine coupling of a ^{133}Cs nucleus; its g factor is slightly smaller (Table 1) than that of the primary spectrum. The pattern of this secondary spectrum points to a species of lower symmetry, *i.e.*, C_{2v} or C_2 (see below).

It is a common phenomenon that the concentration of the alkali-metal cations increases upon prolonged contact with the metal mirror;[14] this is borne out by the observation that the reduction periods depend strongly on the starting concentration of neutral **2**: the lower the concentration of **2** the shorter is the reduction period necessary to produce the EPR spectrum mirroring the C_2 (or C_{2v}) symmetry.

Thus, the EPR spectrum indicating C_2 (or C_{2v}) symmetry is connected with an increase of the counterion concentration which promotes the formation of contact ion pairs.

In MTHF as the solvent, even after short reduction periods EPR and ENDOR spectra monitoring exclusively C_2 (or C_{2v}) symmetry of $2^{\bullet -}$ are recorded. This is demonstrated in the EPR spectrum of $2^{\bullet -}$–Cs^+–MTHF (Fig. 3). The spectral pattern is dominated by the 0.12 mT splitting of the ^{133} Cs nucleus into eight equidistant lines (Table 1) due to ion-pair formation. For K-reduced $2^{\bullet -}$ the $^{39}K^+$ coupling constant can be estimated from the simulations to be < 0.01 mT. The ratio of these coupling constants is in agreement with the theoretical values[12] on the assumption that the spin population at the metal cations is almost identical for K^+ and Cs^+ ion pairs (Table 1).

Temperature Dependence of the EPR Spectra.—Fig. 4 shows the EPR spectra of $2^{\bullet -}$–Cs^+–THF after a 10 min reduction at temperatures between 178 and 223 K. At 178 K the EPR signal is governed by the primary spectrum but the pattern of the broader superimposed component (see above) is already discernible. The higher the temperature, the more the pattern of the broader spectrum becomes dominant. This behaviour is fully reversible upon cooling or heating the sample.

ENDOR spectra taken with the field locked at two different positions of the EPR signal at 198 K[15] (Fig. 5) present the coupling constants belonging to the two spectra. The ENDOR spectrum taken from the middle of the EPR spectrum indicates four proton coupling constants, a_H, of 0.014, 0.097, 0.131 and 0.165 mT, as well as a coupling constant of ^{133}Cs [0.116 mT; Fig. 5(*b*)]. The ENDOR spectrum with the magnetic field locked at

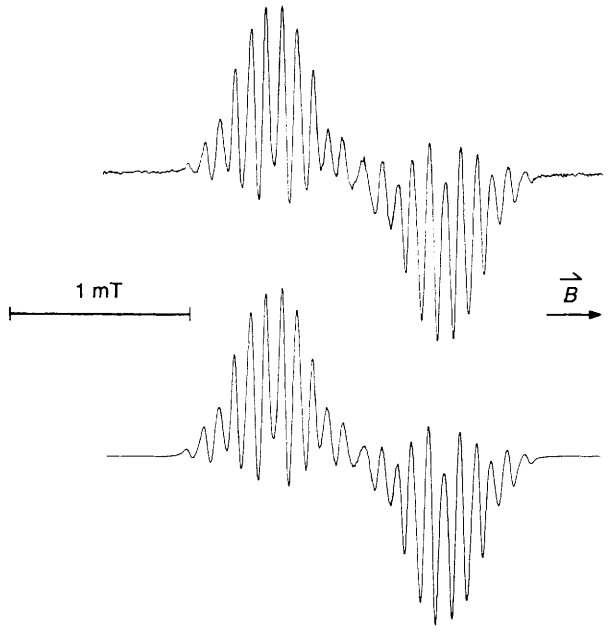

Fig. 3 EPR spectrum of $\mathbf{2}^{\bullet -}$ (solvent, MTHF; counterion Cs^+; T = 198 K) and its simulation (below)

the wing of the EPR signal only shows a_H of 0.013, 0.097 and 0.165 mT and that of the ^{133}Cs nucleus. The coupling constants of 0.014 (8 H) and 0.131 (8 H) mT are identical with those found for $\mathbf{2}^{\bullet -}$.[9-11] The simulations demonstrate that the second spectrum is due to the coupling constants of 0.165 mT (4 H), 0.097 mT (4 H), 0.013 mT (4 or 8 H)* as well as the coupling with one ^{133}Cs nucleus (m_I = 7/2) of 0.116 mT which is the reason for the increased width of the EPR spectra (7 × 0.116 ≈ 0.8 mT). The latter spectrum is identical with that detected for $\mathbf{2}^{\bullet -}$–Cs^+–MTHF (Fig. 3). The composition of the EPR signals at different temperatures and the coupling constants are given in Table 1.

The increase of temperature decreases the coordination ability of the solvents and thus promotes the formation of contact ion pairs.[16] Therefore, the above observations again strongly support that ion pairs are the source of the EPR spectra mirroring C_2 (or C_{2v}) symmetry.

Moreover, the lower g factors determined for the EPR spectra reflecting the reduced symmetry are characteristic for radical ions forming ion pairs.[17]

Structure of the Ion Pairs.—It is noteworthy that the proton coupling constants in the EPR spectra indicating C_2 (or C_{2v}) symmetry are independent of the counterion (K^+ or Cs^+, Table 1). This indicates that the different alkali-metal cations form the same ion pair with $\mathbf{2}^{\bullet -}$. The sum of the proton coupling constants is almost identical for both EPR-spectral types [D_{2d} and C_2 (or C_{2v}) symmetry]; therefore it is appropriate that a redistribution of the charge and the spin density accompanies ion-pair formation. This is in line with the contact-ion-pair structure as depicted in Fig. 6. The tub shape of **2** is preserved but the metal cation resides on the twofold symmetry axis of the radical anion (on the hyperfine timescale).

Based on AM1[18] calculations, the space between two facing benzene rings is large enough to encompass a K^+ or Cs^+ ion (Fig. 6). Consequently the symmetry is lowered to C_{2v} and the charge and electron density at the two benzene rings facing the cation is increased relative to that of the metal-free moiety.

* The multiplicity of the small a_H of 0.013 mT cannot be unambiguously established from the simulations of the EPR spectra because of the broad EPR lines.

Table 2 Calculated and experimental proton-hyperfine coupling constants (mT) for $\mathbf{2}^{\bullet -}$ assuming D_{2d} and C_{2v} symmetry (for numbering, see Fig. 7)

Position	Calc. (D_{2d})	Experimental	Calc. (C_{2v})	Experimental
1,4,9,12	0.020	0.018	0.05	0.013
5,8,13,16	0.020	0.018	0.01	0.013 or 0.0
2,3,10,11	0.120	0.130	0.17	0.165
6,7,14,15	0.120	0.130	0.10	0.097

Such a structure can be readily 'modelled' by HMO calculations which take into account the influence of the alkali-metal counterion. For the stabilisation of negative charge by metal association at the centres C(2), C(3), C(10) and C(11) h = +0.3[19] and for the weaker interaction with the counterion at C(1), C(4), C(9) and C(12) h = +0.15 was chosen (Fig. 7). The non-planarity of the π system was mimicked by weakening the interaction between the benzene rings (k = 0.85). The agreement between the thus calculated and the experimental coupling constants is satisfactory (Table 2). The $a_{H(2,3,6,7,10,11,14,15)}$ of 0.13 mT (8 H, calc. 0.12 mT) in free-ion $\mathbf{2}^{\bullet -}$ is split into the $a_{H(2,3,10,11)}$ of 0.165 mT (4 H, calc. 0.17 mT) and $a_{H(6,7,14,15)}$ 0.097 mT (4 H, calc. 0.10 mT) in the ion pair. The average value for the two four-proton coupling constants is 0.131 mT, *i.e.*, identical with the larger coupling constant of the free ion. The small $a_{H(1,4,5,8,9,12,13,16)}$ of 0.014 mT (8 H, calc. 0.02 mT) remains almost constant (0.013 mT; calc. $a_{H(1,4,9,12)}$: 0.05 mT, $a_{H(5,8,13,16)}$: 0.01 mT). This verifies that the overall spin population in $\mathbf{2}^{\bullet -}$ is unsymmetrically distributed between the two benzene rings associated with the metal cation (increased population) and the two 'metal-free' benzene rings.

Comparison with Published Work.—Starting with the dianion of **2**, generated by exhaustive reduction with K metal in MTHF as the solvent, the radical anion of **2** was observed during photo-oxidation with a high-pressure Hg lamp.[9,10] The EPR spectrum taken under these conditions is identical with our spectra ($\mathbf{2}^{\bullet -}$–K^+–THF or MTHF) obtained after a long reduction period, however, without the necessity of irradiation (the results described in refs. 9 and 10 were perfectly reproducible in our hands).

The structure of the dianion $\mathbf{2}^{\bullet -}$ was described as being composed of two 'biphenyl entities' and possessing C_2 symmetry. Based on this assumption and on the lowered symmetry deduced from the EPR spectra of $\mathbf{2}^{\bullet -}$ obtained after photo-oxidation such a bis(biphenylene) structure was also postulated for the radical anion. Thus the two different structures of $\mathbf{2}^{\bullet -}$ must be separated by a remarkably high activation barrier which disappears in the neutral stage of **2** because upon reoxidation, unaltered **2** is recovered.[8]

We performed AM1 calculations[18] for **2**, $\mathbf{2}^{\bullet -}$ and $\mathbf{2}^{2-}$ starting from different geometries, *i.e.*, the tub-shaped neutral and various bent bis(biphenylene)-like structures. For none of the starting geometries did the semiempirical geometry-optimization procedures yield a bis(biphenylene)-like structure (Fig. 1) as the minimum. The optimised structure for $\mathbf{2}^{2-}$ established a slightly flattened, tub-shaped geometry; for the radical anion, the flattening was less marked.

Conclusions

Taking our results and the AM1 calculations in ref. 11 into account, the bent bis(biphenylene) structure for the one- and two-electron reduced stages of tetraphenylene, $\mathbf{2}^{\bullet -}$ and $\mathbf{2}^{2-}$,

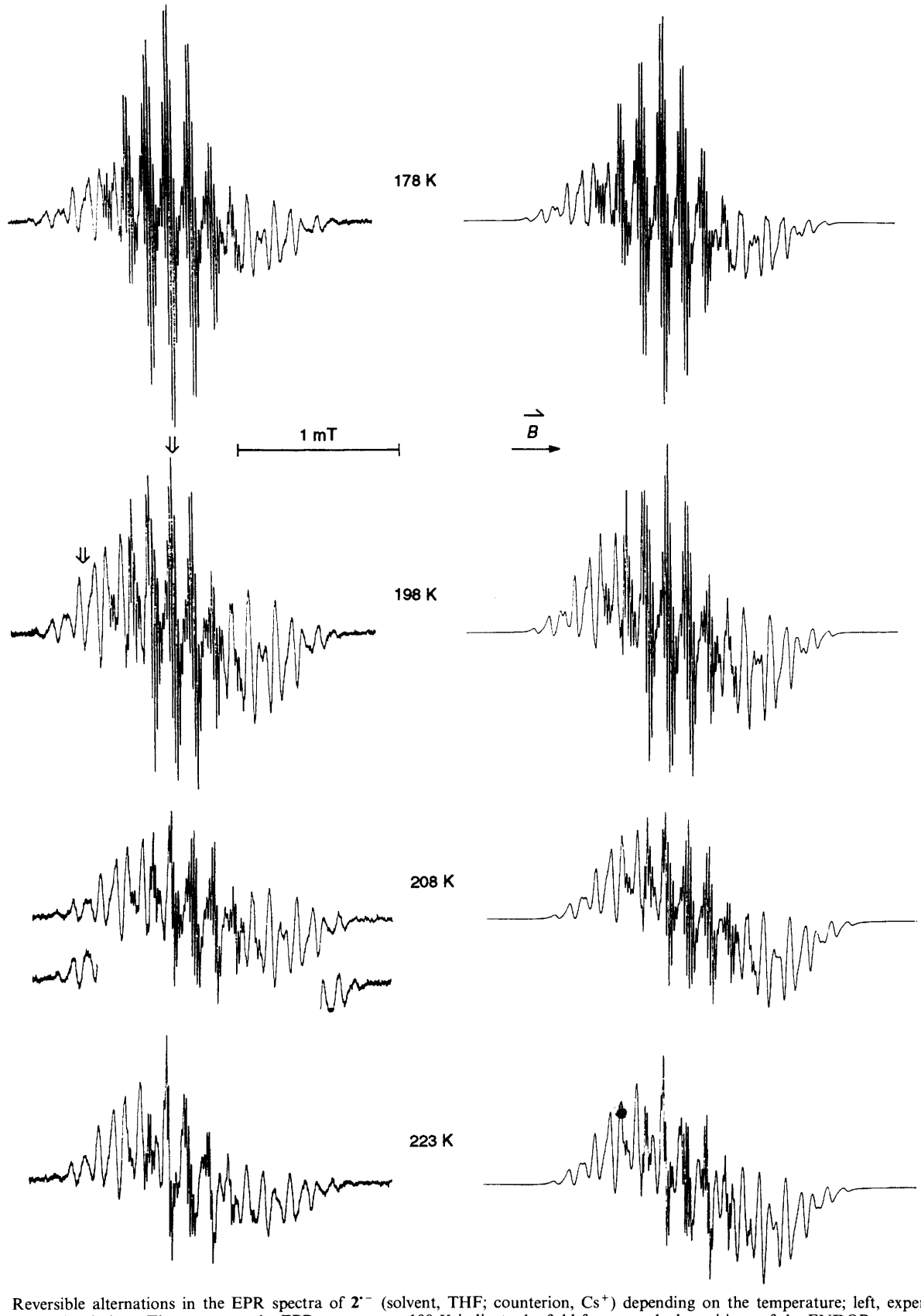

Fig. 4 Reversible alternations in the EPR spectra of $2^{\bullet -}$ (solvent, THF; counterion, Cs^+) depending on the temperature; left, experimental spectra; right, simulations. The arrows at the EPR spectrum at 198 K indicate the field-frequency-lock positions of the ENDOR spectra shown in Fig. 5.

does not seem to be an appropriate rationalisation of the decrease of symmetry monitored by EPR and NMR spectroscopy, respectively.

An interpretation of the previous results[9,10] in the light of our findings draws the following picture. The radical anion $2^{\bullet -}$ forms contact ion pairs with K^+ and Cs^+. The equilibrium between the free ion of $2^{\bullet -}$ and the contact ion pairs is strongly dependent on the concentration ratio of **2**, $2^{\bullet -}$ (2^{2-}) and the

metal cations in solution. Upon complete reduction of **2** to the dianion $\mathbf{2}^{2-}$–2 M^+ followed by photo-oxidation, there is an excess of metal cations in solution and formation of the contact ion pair $\mathbf{2}^{\bullet-}$–M^+ of C_{2v} symmetry is advanced. This is verified by an experiment in which we had added $NaB(Ph)_4$ to Na-reduced $\mathbf{2}^{\bullet-}$: the increased Na^+ concentration leads to an immediate observation of the EPR/ENDOR spectrum belonging to C_{2v}-symmetric $\mathbf{2}^{\bullet-}$.

The EPR spectra indicate the presence of one counterion; triple-ion formation as established for the cyclooctatetraene radical anion formed by photoionisation in rigid media[20] cannot be deduced from our spectra.

To summarise, our results strongly support ion pair formation with the alkali-metal cations K^+ and Cs^+ as the crucial factor of the symmetry reduction in $\mathbf{2}^{\bullet-}$ instead of the formation of a twisted structure. The reason why ion-pair formation was overlooked in refs. 9 and 10 may be the rather small coupling constant of the $^{39}K^+$ counterion (see above). Moreover it seems likely that the reduced symmetry of $\mathbf{2}^{2-}$, as shown by NMR spectroscopy,[8] may also result from counterion interaction.*

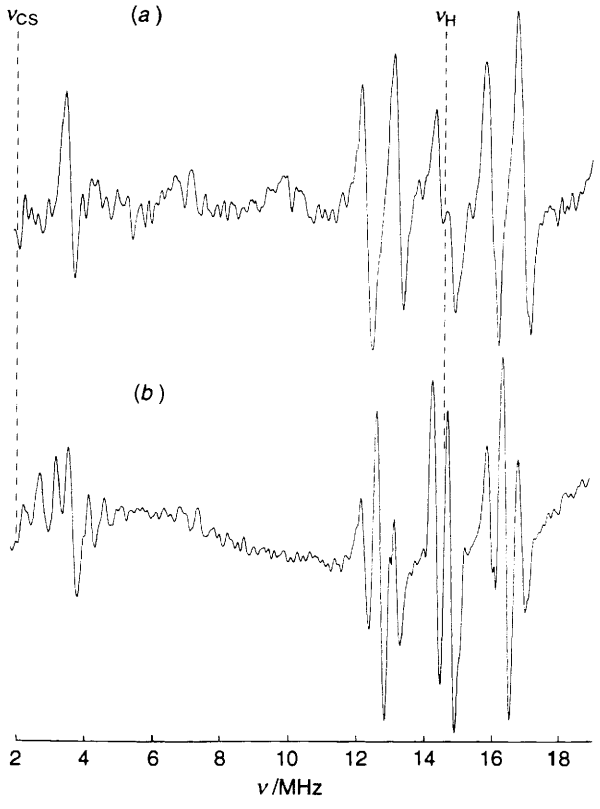

Fig. 5 ENDOR spectra of $\mathbf{2}^{\bullet-}$ (solvent, THF; counterion Cs^+; T = 198 K) taken at two positions of the EPR spectrum. For the upper ENDOR spectrum (*a*) the field-frequency-lock position is at the low-field wing of the EPR signal, for the lower (*b*) it is at the centre, see arrows in Fig. 4.

Appendix

Electronic Spectra.—Hitherto, the electronic absorption spectra of $\mathbf{2}^{\bullet-}$ and $\mathbf{2}^{2-}$ have not been reported. As we are able to measure simultaneously EPR and absorption spectra in the visible region[21] we here present the data for the two ions. The colourless solutions of neutral **2** turned purple-red after the reduction process. Accordingly a broad absorption at 570–580 nm was observed. Upon exhaustive reduction, so that no EPR spectrum could be detected, a band at 670 nm was detected; this could be ascribed to the dianion. The maxima are to some extent dependent upon the solvent, the counterion and the temperature, however, because of the large widths of the bands, it is not appropriate to discuss the solvatochromism.

Acknowledgements

We are obliged to Professor A. G. Davies (University College, London) for fruitful discussions and encouragement and thank

* It would be interesting to attempt to isolate $\mathbf{2}^{2-}$–2 K^+, and to determine the structure by X-ray diffraction, as has been done for $\mathbf{1}^{2-}$–2 K^+.[4]

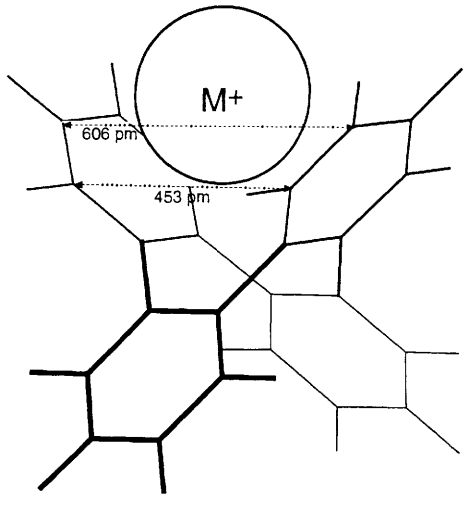

Fig. 6 Ion-pair structure of $\mathbf{2}^{\bullet-}$–M^+ (M = Na, K, Cs) deduced from EPR spectra

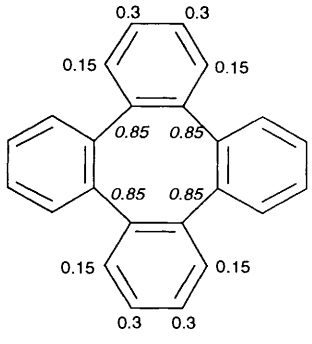

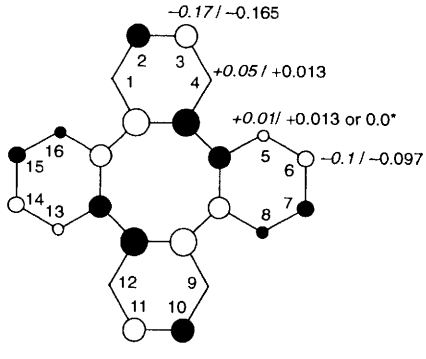

Fig. 7 Parameters (left), numbering and HMO-calculated *vs.* measured a_H (right, calc. *italic*) for $\mathbf{2}^{\bullet-}$–M^+ (because of the small calculated and experimental value of a_H for H(1,4,9,12) and H(5,8,13,16) an unambiguous assignment and determination of the multiplicity was not possible, see also the text)

Mr. C. Burda for experimental assistance. This work was supported by the Swiss National Science Foundation. G. G. is indepted to the *Treubel Fonds* of the *Freiwillige Akademische Gesellschaft*, Basel, for a scholarship.

References

1 K. Müllen, *Chem. Rev.*, 1984, **84**, 603; K. Müllen, W. Huber, G. Neumann, C. Schnieders and H. Unterberg, *J. Am. Chem. Soc.*, 1985, **107**, 801; K. Müllen, *Pure Appl. Chem.*, 1986, **58**, 177; D. Gust, G. H. J. Senkler and K. Mislow, *J. Chem. Soc., Chem. Commun.*, 1972, 1345.
2 R. Willstätter and E. Waser, *Ber. Dtsch. Chem. Ges.*, 1911, **44**, 3423; R. Willstätter and M. Heidelberger, *Ber. Dtsch. Chem. Ges.*, 1913, **46**, 517.
3 R. A. Raphael in *Non-Benzenoid Aromatic Compounds*, ed. D. Ginsburg, Interscience, New York, 1959.
4 N. Hu, L. Gong, Z. Jin and W. Chen, *J. Organomet. Chem.*, 1988, **352**, 61.
5 H. Kojima, A. J. Bard, H. N. C. Wong and F. Sondheimer, *J. Am. Chem. Soc.*, 1976, **98**, 5560; K. Müllen, *Helv. Chim. Acta*, 1978, **61**, 1296.
6 F. Gerson, W. B. Martin, G. Plattner, F. Sondheimer and H. N. C. Wong, *Helv. Chim. Acta*, 1976, **59**, 2038.
7 I. L. Karle and L. O. Brockway, *J. Am. Chem. Soc.*, 1944, **66**, 1974.
8 W. Huber, A. May and K. Müllen, *Chem. Ber.*, 1981, **114**, 1318.
9 W. Huber, *Tetrahedron Lett.*, 1985, **26**, 181.
10 W. Huber and K. Müllen, *Acc. Chem. Res.*, 1986, **19**, 300.
11 D. V. Avila, A. G. Davies, M. L. Girbal and K. M. Ng, *J. Chem. Soc., Perkin Trans. 2*, 1990, 1693.
12 J. R. Morton and K. F. Preston, *J. Magn. Reson.*, 1978, **30**, 577.
13 C. Reichardt, *Solvents and Solvent Effects in Organic Chemistry*, VCH, Weinheim, 1988.
14 F. Gerson, M. Scholz, A. de Meijere, B. König, J. Heinze and K. Meerholz, *Helv. Chim. Acta*, 1992, **75**, 2307; F. Gerson, B. Kowert and B. M. Peake, *J. Am. Chem. Soc.*, 1974, **96**, 118.
15 H. Kurreck, B. Kirste and W. Lubitz, *Electron Nuclear Double Resonance Spectroscopy of Radicals in Solution*, VCH, Weinheim, 1988.
16 T. Takeshita and N. Hirota, *J. Am. Chem. Soc.*, 1971, **93**, 6421; M. Szwarc, *Ions and Ion Pairs in Organic Reactions*, Wiley, New York, London, Sydney, Toronto, 1972.
17 W. G. Williams, R. J. Pritchett and G. K. Fraenkel, *J. Chem. Phys.*, 1970, **52**, 5584.
18 M. J. S. Dewar, E. G. Zoebisch, E. F. Healy and J. J. P. Stewart, *J. Am. Chem. Soc.*, 1985, **107**, 3902.
19 E. Heilbronner and H. Bock, *The HMO-Model and its Application*, Wiley and Verlag Chemie, London, New York and Weinheim, 1976.
20 V. Dvorak and J. Michl, *J. Am. Chem. Soc.*, 1976, **98**, 1080.
21 G. Gescheidt, submitted for publication to *Rev. Sci. Inst.*

Paper 3/07458G
Received 20*th December* 1993
Accepted 31*st January* 1994